

CHSH Bell Tests For Optical Hybrid Entanglement

Morteza Moradi,¹ Juan Camilo López Carreño,^{2,1} Adam Buraczewski,¹ Thomas McDermott,¹
Beate Elisabeth Asenbeck,³ Julien Laurat,³ and Magdalena Stobińska^{1,*}

¹*Institute of Informatics, Faculty of Mathematics, Informatics and Mechanics,
University of Warsaw, Banacha 2, 02-097 Warsaw, Poland*

²*Institute of Theoretical Physics, Faculty of Physics, University of Warsaw, Pasteura 5, 02-093 Warsaw, Poland*

³*Laboratoire Kastler Brossel, Sorbonne Université, CNRS,
ENS-Université PSL, Collège de France, 4 Place Jussieu, 75005 Paris, France*

(Dated: June 10, 2024)

Optical hybrid entanglement can be created between two qubits, one encoded in a single photon and another one in coherent states with opposite phases. It opens the path to a variety of quantum technologies, such as heterogeneous quantum networks, merging continuous and discrete variable encoding, and enabling the transport and interconversion of information. However, reliable characterization of the nature of this entanglement is limited so far to full quantum state tomography. Here, we perform a thorough study of Clauser–Horne–Shimony–Holt (CHSH) Bell inequality tests, enabling practical verification of quantum correlations for optical hybrid entanglement. We show that a practical violation of this inequality is possible with simple photon number on/off measurements if detection efficiencies stay above 82%. Another approach, based on photon-number parity measurements, requires 94% efficiency but works well in the limit of higher photon populations. Both tests use no postselection of the measurement outcomes and they are free of the fair-sampling hypothesis. Our proposal paves the way to performing loophole-free tests using feasible experimental tasks such as coherent state interference and photon counting, and to verification of hybrid entanglement in real-world applications.

I. INTRODUCTION

Optical hybrid entanglement is a form of quantum correlations that embodies the original Schrödinger’s *Gedankenexperiment* [1] by replacing the cat with a classical light beam, i.e. a single photon is entangled with a coherent light [2–5]. It may become a key asset in resource-efficient quantum computation [6], quantum key distribution [7–9] and quantum buses [10, 11]; it has already been employed in complex protocols which paved the way to building heterogeneous quantum networks, e.g., entanglement swapping, and a quantum encoding converter [12, 13]. Furthermore, it was used to probe fundamental limits of quantum theory [14, 15], studying hybrid discrete- (DV) and continuous-variable (CV) quantum information [5, 16], and the information capacity of a photonic state [17].

Quantum technologies often require testing of quantum nonlocality in underlying resources and this is particularly challenging for optical hybrid entanglement. Its dual DV–CV nature implies that Bell nonlocality tests based on hybrid measurement strategies should be optimal. They involve a binary observable measured on the single photon mode and one with a continuous spectrum on the other mode. However, since implementing random Bell test settings in the photon number basis is not experimentally possible, strategies harnessing general qubit measurements are impractical. More universal approaches often employ coarse-graining of detection outcomes for multiphoton entanglement, which can impair Bell nonlocality tests [18, 19]. Moreover, hybrid quantum states decohere exponentially fast with the increasing photon population of the classical light wave [16, 20, 21]. Therefore, how to de-

sign a nonlocality test for hybrid entanglement that can be set up in a laboratory, remains an open question.

Until now, nonlocality tests based on quantum steering inequality [22] and several strategies based on the Clauser–Horne–Shimony–Holt (CHSH) Bell inequality [23] have been outlined. In [24], the nonlocality of hybrid entanglement was tested with displaced parity measurements on both modes. A hybrid detection strategy was also discussed where the measurement on DV mode was replaced with a general qubit measurement. These tests need detection efficiencies of at least 90%. In [25], two hybrid strategies were considered, that involved either displaced parity or displaced on/off measurements. There, the minimal required detection efficiency is 83% for the former, and 63% for the latter test, respectively. However, performing a qubit rotation in the photon-number basis is currently challenging.

Other optical hybrid Bell tests, e.g. hybrid polarization entanglement [26], can serve as a guideline. Although this state is physically different from the photon-number entanglement we consider, it shows mathematical similarities. The hybrid nonlocality testing strategies proposed for it involve displaced parity and displaced on/off measurements for the CV mode and a generalized polarization measurement for the DV mode. Albeit they can be implemented with polarizers and photon-number-resolving (PNR) detection of efficiencies higher than 82%, these Bell tests have not been performed yet.

Here, we perform a thorough analytical and numerical study of two practical CHSH Bell inequality tests possessing a high potential to achieve feasible verification of quantum nonlocality in the optical hybrid entanglement. They can be implemented in an experimental setup, where each mode interferes with a coherent field followed by on/off or parity measurements, realized by means of e.g. PNR detectors [27]. We show that the first test can achieve the inequality violation for detection efficiencies higher than 82% and amplitudes of the

* magdalena.stobinska@gmail.com; Corresponding author

CV mode below 0.6. In the ideal, lossless conditions, this test would allow for a violation of up to 2.71. In contrast, the latter measurement scheme works with higher amplitudes but also sets higher requirements for system efficiencies, which must stay above 94%. This renders it less practical. Finally, for comparison, we also consider hybrid tests, modified for general qubit measurements, and show that in theory, this flavor of hybrid entanglement can maximally violate the CHSH Bell inequality. All the analyzed measurement schemes do not involve postselection and therefore, they have the capability to keep the detection loophole closed.

This paper is organized as follows. Section II briefly discusses the definition of optical hybrid entanglement as considered in this study as well as its basic properties. In Section III we introduce a general Bell test design based on the CHSH Bell inequality, including the experimental setup, model of losses used, and the theoretical background. Next, in Section IV we present and discuss numerical results obtained by applying various measurement schemes for the nonlocality tests. Section V is devoted to an outlook and conclusions.

II. OPTICAL HYBRID ENTANGLEMENT

Let us consider the following hybrid entanglement that was recently generated [3] and subsequently used in various protocols [12, 13, 28, 29]

$$|\Psi\rangle = \frac{1}{\sqrt{2}}(|0\rangle_A |\text{cat}^-\rangle_B + |1\rangle_A |\text{cat}^+\rangle_B). \quad (1)$$

In mode A , a discrete-variable qubit is encoded in photon-number states $|0\rangle$ and $|1\rangle$ – the vacuum and single-photon Fock state, respectively. The qubit is entangled with mode B that carries two mutually orthogonal continuous-variable states, $|\text{cat}^-\rangle$ and $|\text{cat}^+\rangle$. Both of them are superpositions of coherent states of the same amplitude but opposite phases

$$|\text{cat}^\pm\rangle = \frac{1}{N_\pm}(|\gamma\rangle \pm |-\gamma\rangle), \quad (2)$$

where $N_\pm = \sqrt{2(1 \pm e^{-2|\gamma|^2})}$ is the normalization constant and $|\gamma\rangle = e^{-\frac{|\gamma|^2}{2}} \sum_{n=0}^{\infty} \frac{\gamma^n}{\sqrt{n!}} |n\rangle$ is a coherent state. States $|\text{cat}^\pm\rangle$ are orthogonal, $\langle \text{cat}^+ | \text{cat}^- \rangle = 0$, which stems from the fact that $|\text{cat}^+\rangle$ carries only even photon-number components while $|\text{cat}^-\rangle$ only odd ones. This property works as a hint that PNR-based measurement schemes could be the best suited for their discrimination.

Full characterization of $|\Psi\rangle$ was realized using efficient quantum state tomography [3] and quantum steering tests were also performed [22]. However, a full nonlocality test has not been carried out yet. Interestingly, in the limit of $\gamma \rightarrow 0$, $|\Psi\rangle$ tends to the single-photon entanglement $\frac{1}{\sqrt{2}}(|0\rangle |1\rangle - |1\rangle |0\rangle)$.

Also in this case verification of nonlocality and entanglement in $|\Psi\rangle$ is conceptually challenging and it has generated a lot of attention [30–35].

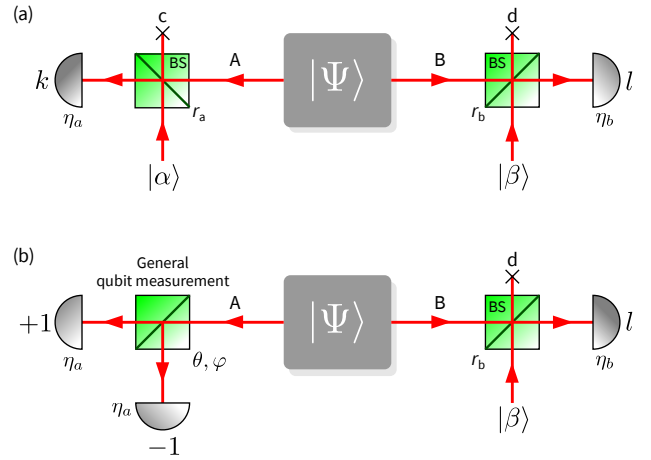


FIG. 1. Nonlocality Bell tests for an optical hybrid bipartite photon-number entanglement $|\Psi\rangle$, as defined in Eq. (1). (a) Two modes of the state are locally interfered with coherent fields, $|\alpha\rangle$ and $|\beta\rangle$, followed by measurements of efficiency η_a and η_b . Here, the variable beam splitters' reflectivities r_a and r_b act as the Bell test settings. The registered readouts k and l are coarse-grained into the binary outcomes of on/off or even/odd measurements used in the CHSH Bell inequality (3). (b) Tests with hybrid measurement strategy, where a measurement on mode A is replaced by a general qubit measurement.

III. GENERAL BELL TEST DESIGN FOR OPTICAL HYBRID ENTANGLEMENT

Verification of quantum nonlocality requires designing a viable Bell test, a task that is quantum state-specific [36, 37]. However, universal methods for finding a well-matched one are not known. Moreover, experimental implementations of Bell tests are limited by the number of accessible measurement strategies, which in the case of photonic setups comprise polarization rotations, displacement operations, homodyne, and detectors of high efficiency, e.g., superconducting nanowires [38] or transition-edge sensors [39]. Furthermore, within the current state of the art, the implementation of rotations in the Fock state basis, which will result in the creation of superpositions of states with different photon numbers, is challenging.

The CHSH Bell inequality, which facilitated the first loophole-free Bell tests [40, 41], takes the form

$$S = \langle A_1 B_1 \rangle + \langle A_1 B_2 \rangle + \langle A_2 B_1 \rangle - \langle A_2 B_2 \rangle \leq 2, \quad (3)$$

where A_i (B_i), for $i = 1, 2$, are binary observables of values ± 1 , measured on mode A (B). It was successful because of its robustness against noise and errors in experimental settings. Quantum correlations allow S to achieve values up to $2\sqrt{2} \approx 2.83$ and subsequently violate inequality (3). Thus, observing CHSH values clearly crossing the classical boundary of 2 is the goal of any practical test.

We propose to employ the CHSH inequality and either on/off or parity measurements for testing optical hybrid entanglement. In Fig. 1(a), two modes of the shared state $|\Psi\rangle$ are

locally interfered with coherent fields, $|\alpha\rangle$ and $|\beta\rangle$, followed by measurements of efficiency $0 < \eta_{a,b} \leq 1$. The variable beam splitters' reflectivities r_a and r_b act as the Bell test settings. The registered readouts k and l are then coarse-grained into two sets, either zero/non-zero or even/odd numbers of photons (Sections IV A and IV B).

This design builds on a group theory result that maps two-mode Fock states $|n\rangle|\Sigma - n\rangle$ to Dicke spin- $\frac{\Sigma}{2}$ states with component $S_z = \frac{\Sigma}{2} - n$, by means of the Schwinger representation [42]. Next, we observe that any arbitrary rotation of S_z -spin component encoded in a product of Fock states is easily implemented by means of Fock state interference on a beam splitter [43]. Reflectivities set the spin rotation angles. We also note the fact that testing photon-number correlations requires erasing ‘how-many-photons’ information before taking measurements. This step requires that we locally interfere each mode of the photon-number entangled state with a quantum superposition of indefinite number of photons, e.g., a coherent state, not merely with a Fock state. Effectively, if we examine this interference in the Fock state basis, it will amount not only to the spin rotation, but also to varying the spin value $\frac{\Sigma}{2}$ each time the measurements are taken. In this way, in the Bell test, we no longer need to perform rotations directly in the Fock state basis, but we carry out rotations of a spin that fluctuates in length instead. These Bell tests can detect nonlocality in a wide class of bipartite entanglement: squeezed vacuum, single-photon entanglement, entangled coherent states, and generalized Holland-Burnett states [24, 44–49].

In Fig. 1(b) we further modify the setup from Fig. 1(a) for generalized qubit measurements in mode A . The goal is to see how much improvement such a test can offer (Sections IV C and IV D). To this end, we assume that the above-mentioned rotations are experimentally feasible.

To investigate the collective effect of losses in the state generation, transmission, and imperfect detection in full optical tests, we model them with a beam splitter of transmittivity $\eta_{a,b}$ inserted in front of each detector. In hybrid Bell tests, we avoid the post-selection loophole by assigning the value +1 to the measurement outcome of observable A_i if a ‘no-detection’ event in mode A occurs, i.e. the effective observable could be written as $A_i^{\text{eff}} = \eta A_i + (1 - \eta)\mathbb{1}$.

We also notice that for the homodyne limit (HD), characterized by very small reflectivities, $r_a, r_b \rightarrow 0$, and large amplitudes of the coherent fields, $|\alpha|^2, |\beta|^2 \rightarrow \infty$, the beam splitter interference may be approximated with displacement operators $D(\delta_{\alpha,\beta})$ with $\delta_\alpha = -i\alpha\sqrt{r_a}$ and $\delta_\beta = -i\beta\sqrt{r_b}$ [50, 51]. In this case, these displacements become the measurement settings. However, in this limit, the photon population of the local oscillators is several orders of magnitude larger than that of the measured state, $|\beta|^2 \gg |\gamma|^2$, which may pose additional experimental challenges, e.g. the PNR detection of large photon numbers [50, 52].

Details of analytical derivations and numerical methods used for obtaining the results presented in Sections IV A–IV D are given in the Supplementary Material.

IV. RESULTS

A. CHSH test with on/off measurements

The first CHSH Bell test that we will outline is based on the scheme shown in Fig. 1(a), where the detection outcomes k and l are split into four sets according to the vacuum and non-vacuum events registered in modes A and B , $\{(k=0, l=0), (k=0, l \neq 0), (k \neq 0, l=0), (k \neq 0, l \neq 0)\}$; they correspond to the binary measurement outcomes $\{(+1, +1), (+1, -1), (-1, +1), (-1, -1)\}$ assigned to A and B , respectively. The on/off measurement operator takes the form

$$\Pi_{\text{on/off}} = |0\rangle\langle 0| - \sum_{n=1}^{\infty} |n\rangle\langle n| = 2|0\rangle\langle 0| - \mathbb{1}, \quad (4)$$

where $\mathbb{1}$ denotes the identity operator. We would like to emphasize that $\Pi_{\text{on/off}}$ describes solely the detection, not the observable employed in the Bell test. It is challenging to concisely analytically express a single observable A_i (or B_j) and to reveal its dependence on the settings of the Bell test (r_a and r_b), but we can write down explicitly the correlation function between these observables as follows

$$\langle A_i B_j \rangle = \text{Tr} \left\{ \Pi_{\text{on/off}}^{(A)} \Pi_{\text{on/off}}^{(B)} \text{Tr}_{c,d} [\mathcal{U}_{\text{BS}}(r_{a_i}) \mathcal{U}_{\text{BS}}(r_{b_j}) \right. \\ \left. \rho_\Psi \rho_\alpha \rho_\beta \mathcal{U}_{\text{BS}}^\dagger(r_{b_j}) \mathcal{U}_{\text{BS}}^\dagger(r_{a_i})] \Pi_{\text{on/off}}^{(B)\dagger} \Pi_{\text{on/off}}^{(A)\dagger} \right\}, \quad (5)$$

where $\rho_\Psi = |\Psi\rangle\langle\Psi|$, ρ_α and ρ_β are the coherent states $|\alpha\rangle$ and $|\beta\rangle$. The action of a beam splitter is described by the unitary $\mathcal{U}_{\text{BS}}(r) = e^{-i\mu(a^\dagger b - ab^\dagger)}$, where $\mu = 2 \arcsin \sqrt{r}$, r is the beam splitter reflectivity and a, b denote the annihilation operators of interfering modes.

To compute the maximal value of parameter S and achieve the CHSH inequality violation for given γ and detection efficiencies $\eta_{a,b}$, we numerically optimize Eq. (3) with the correlation functions given by Eq. (5), with respect to the Bell test settings $r_{a_{1,2}}, r_{b_{1,2}}$ for given parameters α, β . Next, we optimize the amplitudes α, β to obtain the minimal detection efficiencies $\eta_{a,b}$ required for the violation. Numerical optimization is simplified by using the real domain for parameters γ, α and β . This approach is viable as phases can be aligned in the experimental implementation.

The results for the on/off measurements are depicted in Fig. 2. In panel (a) we fix the parameters $\alpha = \beta = 2$ and set equal detection efficiencies $\eta_a = \eta_b$. In the limit $\gamma \rightarrow 0$ and perfect detection ($\eta_{a,b} = 1$) we obtain $S = 2.57$. The value of S gradually drops for higher γ and reaches the boundary $S = 2$ for $\gamma = 0.81$, because the odds of spotting the zero-photon measurement quickly vanishes for highly-occupied states. Observing Bell inequality violation becomes also impossible below $\eta_a = \eta_b = 0.87$. For comparison, when we set higher $\alpha = \beta = 7$, in the limit $\gamma \rightarrow 0$ and perfect detection we obtain maximum violation of $S = 2.69$, the same value we got in Ref. [49] for the single-photon case.

Next, we studied the interplay between the minimal requirements for unequal detection efficiencies. Fig. 2(b) shows the

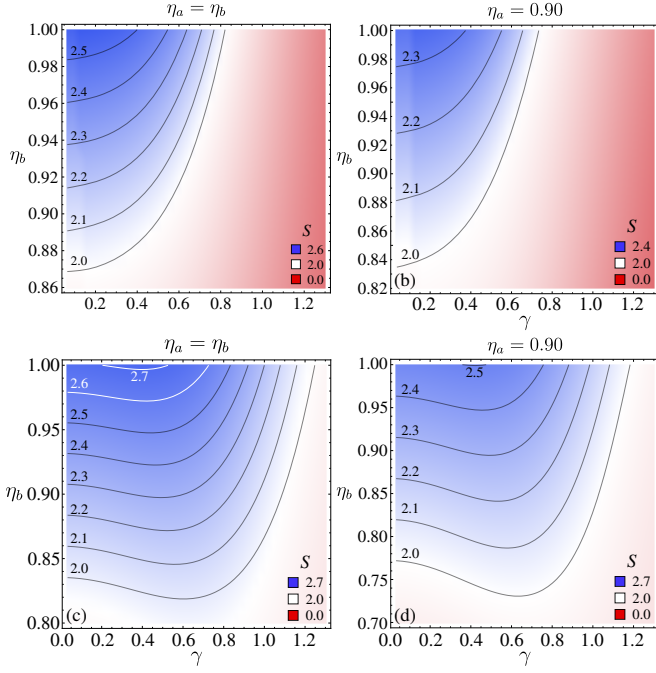


FIG. 2. Violation of the CHSH inequality with on/off measurements computed for the hybrid entanglement $|\Psi\rangle$, as a function of the amplitude γ of the state $|\text{cat}^\pm\rangle$ and (a) equal detection efficiencies in both arms, $\eta_a = \eta_b$ and $\alpha = \beta = 2$, and (b) fixed qubit detection efficiency, $\eta_a = 0.9$ and $\alpha = \beta = 2$. Panels (c) and (d) display the counterparts of panels (a) and (b), respectively, but in the homodyne limit.

violations achieved for $\eta_a = 0.9$ and $\alpha = \beta = 2$. They are observed for $\gamma < 0.75$ and $\eta_b > 0.83$. This gain comes at the expense of lowering the value of maximal violation to $S = 2.35$.

The computation results for the homodyne limit are shown in the lower row of Fig. 2. We first derived an analytical formula for correlation functions and then numerically maximized the S with respect to the Bell test settings $\delta_{\alpha_{1,2}}, \delta_{\beta_{1,2}}$. We found that in this case, in panel (c), the CHSH violation is higher than in panel (a), and it is also observed for a wider span of γ . Furthermore, the maximum value of the violation increases to $S = 2.71$ for $\gamma = 0.4$ and for the settings $\delta_{\alpha_1} = 0.18, \delta_{\alpha_2} = -0.56, \delta_{\beta_1} = 0.17, \delta_{\beta_2} = -0.61$, and the minimum efficiency that still provides violation is $\eta_{a,b} = 0.82$ for $\gamma = 0.6$. Fig. 2(d) displays the CHSH violation for $\eta_a = 0.9$ and it is the counterpart of panel (b) in the homodyne limit. Here, the maximal achieved value is higher than in panel (b), reaching $S = 2.5$ for $\gamma = 0.42$, and the minimal efficiency that still provides violation gets to $\eta_b = 0.73$ for $\gamma = 0.63$.

In summary, our results show that significant CHSH violations can be achieved for hybrid entanglement when performing on/off measurements. Notably, such violations can be reached even when the intensity of the local coherent state is comparable to the photonic occupation of the state under study. We also calculated how S increases in the homodyne limit and showed that we can reach a higher violation in this limit.

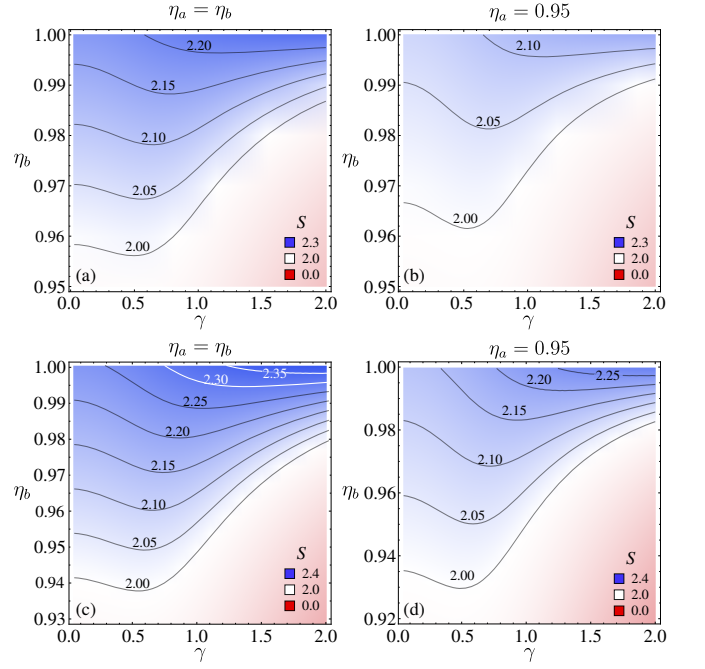


FIG. 3. Violation of the CHSH inequality with parity measurements computed for the hybrid entanglement $|\Psi\rangle$, as a function of the amplitude γ of the state $|\text{cat}^\pm\rangle$ and (a) equal detection efficiencies in both arms, $\eta_a = \eta_b$ and $\alpha = \beta = 1$, and (b) fixed qubit detection efficiency and $\alpha = \beta = 1, \eta_a = 0.95$. Panels (c) and (d) display the counterparts of panels (a) and (b), respectively, but in the homodyne limit.

B. CHSH test with parity measurements

Let us now perform coarse-graining of the measurement results from Fig. 1(a) by assigning -1 to the detection of even numbers of photons ($k = \text{even}$ or $l = \text{even}$), and $+1$ to the detection of odd numbers of photons ($k = \text{odd}$ or $l = \text{odd}$). This strategy mimics the use of parity measurements on modes A and B with

$$\Pi_{\text{parity}} = \sum_{n=0}^{\infty} (-1)^n |n\rangle \langle n|. \quad (6)$$

Following the steps described in Section IV A, we numerically optimize the CHSH value S in Eq. (3) with correlations computed using Eq. (5) but replacing the operator $\Pi_{\text{on/off}}$ with Π_{parity} from Eq. (6).

The results for the parity measurement are shown in Fig. 3. Panel (a) depicts computations for equal efficiencies $\eta_a = \eta_b$. Here $\alpha = \beta = 1$ provide us with the smallest $\eta_{a,b} = 0.96$ for which we see the violations. We find that the maximal CHSH value increases from $S = 2.17$ for $\gamma \rightarrow 0$ to $S = 2.24$ for $\gamma = 2$. We note that these measurements allow to observe violation for larger amplitudes of γ than with on/off measurements. In fact, with this measurement, one could get $S \geq 2$ for $\eta \rightarrow 1$ independently of γ , unlike for the on/off case, where γ was limited. However, parity measurements in general require higher detection efficiencies, because losing a photon can turn an even number of photons into an odd one, and vice versa.

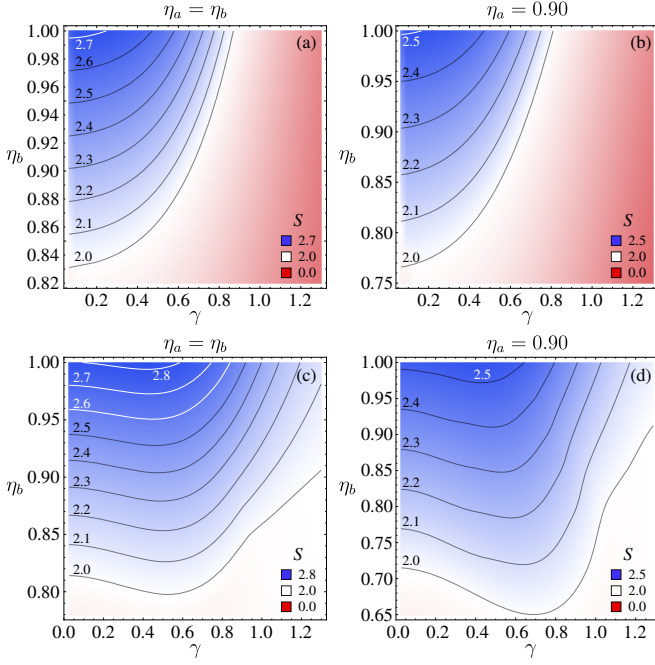


FIG. 4. Violation of the hybrid CHSH Bell test with on/off measurements computed for the hybrid entanglement $|\Psi\rangle$, as a function of the amplitude γ of the state $|\text{cat}^\pm\rangle$ and (a) equal detection efficiencies in both arms, $\eta_a = \eta_b$ and $\alpha = \beta = 2$, and (b) fixed qubit detection efficiency, $\eta_a = 0.9$ and $\alpha = \beta = 2$. Panels (c) and (d) display the counterparts of panels (a) and (b), respectively, but in the homodyne limit.

Fig. 3(b) shows computations for $\eta_a = 0.95$ and $\alpha = \beta = 1$. This efficiency is almost at the minimum necessary for the CHSH violation. Here, $S=2.14$ is reached for $\gamma=2$. A value of η_b required to witness any violation is $\eta_b=0.96$ for $\gamma=0.5$.

In the homodyne limit, the results are shown in panels (c) and (d). For $\eta_a = \eta_b$, panel (c), the violation of $S = 2.39$ is achieved for $\gamma=2$ and it will increase to maximum violation of $S=2.44$ for $\gamma \rightarrow \infty$. However, it very quickly degrades with losses. The lowest efficiency for which $S > 2$ is $\eta_{a,b}=0.94$ for $\gamma=0.54$. In the case of $\eta_a = 0.95$, panel (d), the violation of $S=2.29$ attained for $\gamma=2$, and $S > 2$ is reached for minimum $\eta_b = 0.93$ and $\gamma=0.5$.

Thus, our results show that CHSH violations can also be achieved for hybrid entanglement when performing parity measurements. The magnitudes of the violations are lower than in the on/off case, and require better detection efficiencies, but can be observed at larger values of the amplitude γ . In both cases, the ideal setting which gave us the maximum violation happens in the homodyne limit.

C. Hybrid CHSH test with on/off measurements

Another strategy linked to the specific nature of the considered state is to perform the hybrid Bell test shown in Fig. 1(b). In this design, a general qubit measurement is performed on the single-photon subsystem, while on/off measurements,

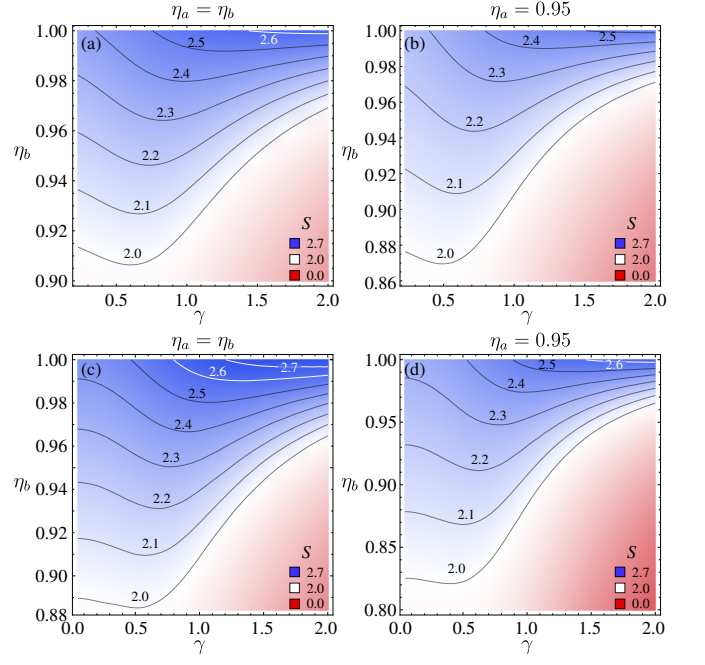


FIG. 5. Violation of the hybrid CHSH Bell test with parity measurements computed for the hybrid entanglement $|\Psi\rangle$, as a function of the amplitude γ of the state $|\text{cat}^\pm\rangle$ and (a) equal detection efficiencies in both arms, $\eta_a = \eta_b$ and $\alpha = \beta = 1$, and (b) fixed qubit detection efficiency, $\eta_a = 0.95$ and $\alpha = \beta = 1$. Panels (c) and (d) display the counterparts of panels (a) and (b), respectively, but in the homodyne limit.

Eq. (4), are applied to mode B . Every qubit observable can be described in terms of Pauli operators σ_X , σ_Y , and σ_Z [53]

$$A_j = \sin \theta_j \cos \phi_j \sigma_X + \sin \theta_j \sin \phi_j \sigma_Y + \cos \theta_j \sigma_Z, \quad (7)$$

where $j = 1, 2$ correspond to two measurement settings used in mode A in the test.

We follow the steps described in Section IV A for the optimization of the CHSH value with the on/off measurements, but we apply the observable defined Eq. (7) in mode A to achieve hybrid inequality. The results are depicted in Fig. 4. Panel (a) is computed for $\alpha = \beta = 2$ and $\eta_a = \eta_b$. Here, $S = 2.72$ is achieved for $\gamma \rightarrow 0$, but CHSH violation is reached only for $\eta_{a,b} \geq 0.82$. The range for which the violation can be observed is bounded by $\gamma=0.88$. Panel (b) displays $\eta_a = 0.9$ for $\alpha = \beta = 2$, for which the maximal violation is $S=2.54$ but the minimal efficiency needed for the violation drops to $\eta_b=0.77$.

In the homodyne limit, the minimal required detection efficiency to observe any CHSH inequality violation is $\eta_{a,b}=0.8$, Fig. 4(c). The highest violation of $S = 2.83$ is obtained for $\gamma = \sqrt{\ln 2}/2 \approx 0.42$. For $\eta_a = 0.9$, panel (d), the minimal η_b equals 0.65 and maximal violation is $S = 2.55$.

The numerical result from panel (c) can be additionally shown analytically using the CHSH rigidity theorem, which states that if a quantum state maximally violates the CHSH inequality, it is equivalent to the maximally entangled Bell pair $\frac{1}{\sqrt{2}}(|0\rangle|0\rangle + |1\rangle|1\rangle)$, while the measurements used are equivalent to the canonical qubit measurements $A_1 = \sigma_Z$, $A_2 =$

σ_X , $B_1 = \frac{1}{\sqrt{2}}(\sigma_Z + \sigma_X)$, $B_2 = \frac{1}{\sqrt{2}}(\sigma_Z - \sigma_X)$ [54, 55]. This prerequisite is fulfilled by $|\Psi\rangle$, because Eq. (1) already possesses the form of a Bell pair. Orthonormal states $|e_0\rangle = |\text{cat}^-\rangle$ and $|e_1\rangle = |\text{cat}^+\rangle$ can be considered as two states of a multiphoton qubit, but they must be complemented by an arbitrary set of orthonormal $|e_i\rangle$ where $i \geq 2$ to form the full basis in an infinite-dimensional Hilbert space.

In order to analytically investigate this theorem, let us take $A_1 = \sigma_Z$ and $A_2 = \sigma_X$, as well as $\delta_{\beta_{1,2}} = \pm\gamma$. With regards to the measurement operators acting on mode B , we note that in the homodyne limit they can be expressed as $B_j = D(\delta_{\beta_j})\Pi_{\text{on/off}}D^\dagger(\delta_{\beta_j}) = 2|\delta_{\beta_j}\rangle\langle\delta_{\beta_j}| - \mathbb{1}$, $j = 1, 2$. In the basis $|e_i\rangle$, they have the following form

$$B_j = \tilde{B}_j \oplus -1, \quad (8a)$$

$$\tilde{B}_j = (-1)^{j-1} \sqrt{1 - e^{-4\gamma^2}} \sigma_X + e^{-2\gamma^2} \sigma_Z, \quad (8b)$$

where $j = 1, 2$. The Supplementary Material details the full proof.

Now, when we substitute $\gamma = \frac{1}{2}\sqrt{\ln 2} \approx 0.42$, then $B_1 = \frac{1}{\sqrt{2}}(\sigma_Z + \sigma_X)$ and $B_2 = \frac{1}{\sqrt{2}}(\sigma_Z - \sigma_X)$ and the maximal violation of the CHSH inequality $S = 2\sqrt{2}$ can be observed, thus proving the CHSH rigidity for the optical hybrid entanglement. This stays in agreement with Ref. [56].

In summary, the hybrid Bell test, in which a general qubit measurement is performed on mode A while mode B is tested with on/off measurements, allows one to achieve higher CHSH inequality violations compared to the case where on/off measurements are performed on both modes. Furthermore, in the homodyne limit, this approach allows one to observe the maximal CHSH violation of $2\sqrt{2}$ for the hybrid entanglement, showing that this state is equivalent to the maximally entangled Bell pair.

D. Hybrid CHSH test with parity measurements

Lastly, we consider a hybrid test in which general qubit measurements, Eq. (7), are performed on mode A , and the parity measurements, Eq. (6), on mode B . Numerical computations follow the steps from Section IV C.

The results are displayed in Fig. 5. Panel (a) is computed for $\alpha = \beta = 1$ and $\eta_a = \eta_b$. Here, the violation reaches $S = 2.62$ for $\gamma = 2$ and drops to $S = 2$ for $\eta_{a,b} = 0.91$ and $\gamma = 0.6$. In the case of $\eta_b = 0.95$, computed for $\alpha = \beta = 1$, panel (b), maximal violation of $S = 2.52$ is reached for $\gamma = 2$. The CHSH inequality is minimally violated for $\eta_b = 0.87$ for $\gamma = 0.45$.

In the homodyne limit, the CHSH parameter computed for $\eta_a = \eta_b$ reaches $S = 2.77$ for $\gamma = 2$, panel (c). The minimum required efficiency is $\eta_a = \eta_b > 0.88$ for $\gamma = 0.47$. For $\eta_a = 0.95$, panel (d), minimal $\eta_b > 0.83$ for $\gamma = 0.37$, while S takes the maximal value of 2.69 for $\gamma \rightarrow \infty$. The CHSH inequality in this case is maximally violated for $\gamma \rightarrow \infty$ and $\eta_{a,b} \rightarrow 1$, which can be also proved analytically. In this limit, $\langle -\gamma|\gamma\rangle = 0$ and

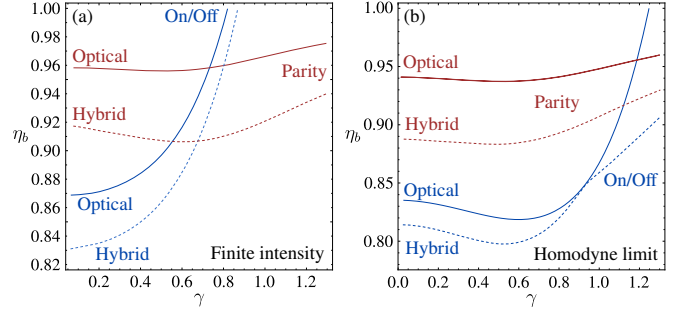


FIG. 6. Comparison of nonlocality CHSH Bell tests for optical photon-number hybrid entanglement, Eq. (1), with various detection strategies: on/off (blue lines) and parity (red line) with full optical (solid lines) and hybrid (dashed lines) measurements. We assume all the measurement devices to be equally efficient, $\eta_a = \eta_b$. The various lines correspond to the thresholds above which CHSH violation is observed when the local interferences (a) have finite intensity and (b) are in the homodyne limit; i.e., the lines are the $S = 2$ isolines from panels (a) and panels (c), respectively, of Figs. 2–5.

observables B_1 and B_2 become

$$B_j = e^{-2|\delta_j|^2} (\cos \varphi_j \sigma_Z - \sin \varphi_j \sigma_Y), \quad (9)$$

where $\varphi_j = 4\gamma \text{Im}(\delta_j)$ and $j = 1, 2$. Then, by substituting $\delta_{\beta_{1,2}} = \pm i\pi/16\gamma$ one gets $B_1 = \frac{1}{\sqrt{2}}(\sigma_Z - \sigma_Y)$ and $B_2 = \frac{1}{\sqrt{2}}(\sigma_Z + \sigma_Y)$, which are the canonical measurements up to a rotation in the X–Y plane. The CHSH inequality can be maximally violated, $S = 2\sqrt{2}$, for $A_1 = \sigma_Z$, $A_2 = \sigma_Y$.

To sum up this case, in analogy to Section IV C, the hybrid CHSH test with parity measurements allows one to achieve higher CHSH Bell inequality violations than the test using parity measurements in both modes, at the expense of the feasibility of the experimental scheme. It also allows one to obtain the maximal violation for a specific set of system parameters.

V. DISCUSSION AND CONCLUSION

We have demonstrated that an optical hybrid entanglement can be practically used to violate a CHSH Bell inequality with available PNR detectors. In the test, each mode of $|\Psi\rangle$, Eq. (1), interferes with a local coherent state $|\alpha\rangle$ and $|\beta\rangle$, respectively, on variable beam splitters of reflectivities r_a and r_b , and subsequently measured. While $r_{a,b}$ act as the Bell test settings, splitting the detection outcomes into two sets of zero and non-zero or even/odd numbers of photons allows us to realize binary on/off measurements. This test requires $|\beta|^2 > |\gamma|^2$ and small finetuned beam splitter reflectivities, otherwise the entanglement is decreased due to correlations with other modes caused by interference. Although the proposed test is challenging to implement due to inevitable losses in the optical paths and imperfect detection, it is within reach of current technology, for example, superconducting-nanowire detectors [38] or transition-edge sensors [39].

For the non-homodyne limit with $\alpha = \beta = 2$ our result is depicted in Figs. 2(a-b), where significant CHSH Bell inequality violations, up to $S = 2.57$, are demonstrated for hybrid entangled state $|\Psi\rangle$ with amplitudes $\gamma < 0.81$, and on/off measurements with detection efficiencies above 0.87. By increasing the value of α, β the optimal Bell value also increases.

Our main result is shown in Figs. 2(c-d) computed for the same on/off measurement but this time in the homodyne limit, i.e. $r_{a,b} \rightarrow 0$ and $\alpha, \beta \rightarrow \infty$, where the local interferences of $|\Psi\rangle$ with coherent states amount to displacement operations [51]. Here we have Bell violations, up to $S = 2.71$ in ideal circumstances, which are demonstrated for states with amplitudes $\gamma < 1.25$, and on/off measurements with detection efficiencies above 0.82. In realistic conditions, for example for $\gamma = 0.44$ and efficiencies $\eta_{a,b} > 0.95$, it gave the Bell violation of $S = 2.51$, which can be obtained with the current experimental setups.

In Fig. 3 we present the result for parity measurement. In the ideal lossless conditions, this allows one to perform the even/odd Bell test for arbitrarily large amplitude γ , reaching the maximal value of $S = 2.44$. However, this measurement is quickly spoiled by losses that remove photons from the state and so these violations are very fragile and vanish quickly by experimental imperfections.

The results presented in Figs. 4–5 are interesting for studying the theory and properties of hybrid entanglement. We enhanced our two measurement strategies with a general qubit measurement performed in the single-photon subsystem. This allowed us to maximally violate the CHSH inequality, up to $S = 2\sqrt{2}$. For example, it lets us decrease the required minimal efficiency of the measurement in the on/off test to $\eta_{a,b} \geq 0.8$ and in the parity test to $\eta_{a,b} \geq 0.88$.

Our numerical computations are summarised in Fig. 6, where we show a comparison of the thresholds above which CHSH violation occurs, as a function of both the detection efficiency, as well as the amplitude γ . Panel (a) displays the lines obtained when the local interference is done with a coherent state with finite intensity, while in panel (b) we show the counterpart in the homodyne limit. In both cases, we find that on/off measurements are most robust to losses, while parity

measurements allow violations for higher values of γ . Moreover, regardless of the type of measurement, the hybrid strategies provide a clear enhancement of the results, lowering the efficiency required to observe CHSH violations. The Supplemental Material includes a table with all the detailed results of the computations.

Our results give interesting insights from both fundamental and technological standpoints. They show ways to study the quantum nonlocality of optical hybrid entangled states, as well as of more general complex bipartite entanglement merging the CV and DV realms.

ACKNOWLEDGMENTS

M.M., A.B. and M.S. were supported by the European Union’s Horizon 2020 research and innovation programme under the Marie Skłodowska-Curie project “AppQInfo” No. 956071. M.S. and A.B. were supported by the National Science Centre “Sonata Bis” project No. 2019/34/E/ST2/00273, the QuantERA II Programme that has received funding from the European Union’s Horizon 2020 research and innovation programme under Grant Agreement No 101017733, project “PhoMemtor” No. 2021/03/Y/ST2/00177, as well as by the Foundation for Polish Science “First Team” project No. POIR.04.04.00-00-220E/16-00 (originally FIRST TEAM/2016-2/17). J.C.L.C. was supported by the Polish National Agency for Academic Exchange (NAWA) under project TULIP with number PPN/U LM/2020/1/00235 and from the Polish National Science Center (NCN) “Sonatina” project CAMEL with number 2021/40/C/ST2/00155. J.L. is a member of the Institut Universitaire de France. This work was supported by the ANR in the framework of France 2030 (ANR-22-PETQ-0011) and via ShoQC project (19-QUAN-0005-05). We gratefully acknowledge Poland’s high-performance computing infrastructure PLGrid (HPC Centers: ACK Cyfronet AGH) for providing computer facilities and support within computational grant no. PLG/2023/016211. We thank A. Mikos-Nuszkiewicz for his discussions.

-
- [1] E. Schrödinger, *Die gegenwärtige Situation in der Quantenmechanik*, *Naturwissenschaften* **23**, 844 (1935).
- [2] H. Jeong, A. Zavatta, M. Kang, S. W. Lee, L. S. Costanzo, S. Grandi, T. C. Ralph and M. Bellini, *Generation of hybrid entanglement of light*, *Nature Photon.* **8**, 564 (2014).
- [3] O. Morin, K. Huang, J. Liu, H. Le Jeannic, C. Fabre, and J. Laurat, *Remote creation of hybrid entanglement between particle-like and wave-like optical qubits*, *Nature Photon.* **8**, 570–574 (2014).
- [4] K. Huang, H. Le Jeannic, O. Morin, T. Darras, G. Guccione, A. Cavaillès, and J. Laurat, *Engineering optical hybrid entanglement between discrete-and continuous-variable states*, *New J. Phys.* **21**, 083033 (2019).
- [5] U. L. Andersen, J. S. Neergaard-Nielsen, P. van Loock, and A. Furusawa, *Hybrid discrete-and continuous-variable quantum information*, *Nature Phys.* **11**, 713 (2015).
- [6] S.-W. Lee and H. Jeong, *Near-deterministic quantum teleportation and resource-efficient quantum computation using linear optics and hybrid qubits*, *Phys. Rev. A* **87**, 022326 (2013).
- [7] J. Rigas, O. Gühne, and N. Lütkenhaus, *Entanglement verification for quantum-key-distribution systems with an underlying bipartite qubit-mode structure*, *Phys. Rev. A* **73**, 012341 (2006).
- [8] C. Wittmann, J. Fürst, C. Wiechers, D. Elser, H. Häsel, N. Lütkenhaus, and G. Leuchs, *Witnessing effective entanglement over a 2 km fiber channel*, *Opt. Express* **18**, 4499 (2010).
- [9] H.-L. Yin and Z.-B. Chen, *Coherent-state-based twin-field quantum key distribution*, *Sci. Rep.* **9**, 14918 (2019).
- [10] T. P. Spiller, K. Nemoto, S. L. Braunstein, W. J. Munro, P. van Loock, and G. J. Milburn, *Quantum computation by communication*, *New J. Phys.* **8**, 30 (2006).

- [11] P. van Loock, W. J. Munro, K. Nemoto, T. P. Spiller, T. D. Ladd, S. L. Braunstein, and G. J. Milburn, *Hybrid quantum computation in quantum optics*, Phys. Rev. A **78**, 022303 (2008).
- [12] G. Guccione, T. Darras, H. Le Jeannic, V. B. Verma, S. W. Nam, A. Cavaillès, and J. Laurat, *Connecting heterogeneous quantum networks by hybrid entanglement swapping*, Sci. Adv. **6**, eaba4508 (2020).
- [13] T. Darras, B.E. Asenbeck, G. Guccione et al., *A quantum-bit encoding converter*, Nat. Photon. **17**, 165–170 (2023).
- [14] Y. Chen, *Macroscopic quantum mechanics: theory and experimental concepts of optomechanics*, J. Phys. B At. Mol. Opt. Phys. **46**, 104001 (2013).
- [15] M. Aspelmeyer, T. J. Kippenberg, and F. Marquardt, *Cavity optomechanics*, Rev. Mod. Phys. **86**, 1391 (2014).
- [16] P. van Loock, *Optical hybrid approaches to quantum information*, Laser Photon. Rev. **5**, 167 (2011).
- [17] I. Nape, B. Ndagano, B. Perez-Garcia, R. I. Hernandez-Aranda, F. S. Roux, T. Konrad, and A. Forbes, *Hybrid entanglement for quantum information and communication applications*. In: Proc. SPIE 10347, *Optical Trapping and Optical Micromanipulation XIV*, 1034711 (25 August 2017).
- [18] M. Stobińska, P. Sekatski, A. Buraczewski, N. Gisin, and G. Leuchs, *Bell-inequality tests with macroscopic entangled states of light*, Phys. Rev. A **84**, 034104 (2011).
- [19] M. Stobińska, F. Töppel, P. Sekatski, and A. Buraczewski, *Towards loophole-free Bell inequality test with preselected unsymmetrical singlet states of light*, Phys. Rev. A **89**, 022119 (2014).
- [20] W. H. Zurek, *Decoherence, Einselection, and the quantum origins of the classical*, Rev. Mod. Phys. **75**, 715 (2003).
- [21] J. Le Jeannic, A. Cavaillès, K. Huang, R. Filip, and J. Laurat, *Slowing quantum decoherence by squeezing in phase space*, Phys. Rev. Lett. **120**, 073603 (2018).
- [22] A. Cavaillès, H. Le Jeannic, J. Raskop, G. Guccione, D. Markham, E. Diamanti, M. D. Shaw, V. B. Verma, S. W. Nam, and J. Laurat, *Demonstration of Einstein–Podolsky–Rosen steering using hybrid continuous- and discrete-variable entanglement of light*, Phys. Rev. Lett. **121**, 170403 (2018).
- [23] J. F. Clauser, M. A. Horne, A. Shimony, and R. A. Holt, *Proposed experiment to test local hidden-variable theories*, Phys. Rev. Lett. **23**, 880 (1969).
- [24] A. Ketterer, *Modular variables in quantum information*, Ph.D. thesis, Université Paris 7, Sorbonne Paris Cité (2016).
- [25] A. Cavaillès, *Non-locality tests and quantum communication protocols using hybrid entanglement of light*, Ph.D. thesis, Sorbonne Université (2019).
- [26] H. Kwon and H. Jeong, *Violation of the Bell–Clauser–Horne–Shimony–Holt inequality using imperfect photodetectors with optical hybrid states*, Phys. Rev. A **88**, 052127 (2013).
- [27] T. Gerrits, N. Thomas-Peter, J. C. Gates, A. E. Lita, B. J. Metcalf, B. Calkins, N. A. Tomlin, A. E. Fox, A. Lamas Linares, J. B. Spring, N. K. Langford, R. P. Mirin, P. G. R. Smith, I. A. Walmsley, S. W. Nam, *On-chip, photon-number-resolving, telecommunication-band detectors for scalable photonic information processing*, Phys. Rev. A **84**, 060301 (2011).
- [28] H. Le Jeannic, A. Cavaillès, J. Raskop, K. Huang, and J. Laurat, *Remote preparation of continuous-variable qubits using loss-tolerant hybrid entanglement of light*, Optica **5**, 1012-1015 (2018).
- [29] R. C. Parker, J. Joo, and T. P. Spiller, *Photonic hybrid state entanglement swapping using cat state superpositions*, Proc. R. Soc. A **476**, 2243 (2020).
- [30] S. M. Tan, D. F. Walls, and M. J. Collett, *Nonlocality of a single photon*, Phys. Rev. Lett. **66**, 252 (1991).
- [31] J. J. Cooper and J. A. Dunningham, *Single particle nonlocality with completely independent reference states*, New J. Phys. **10**, 113024. (2008).
- [32] T. Das, M. Karczewski, A. Mandarino, M. Markiewicz, B. Woloncewicz, and M. Żukowski, *Can single photon excitation of two spatially separated modes lead to a violation of Bell inequality via weak-field homodyne measurements?*, New J. Phys. **23**, 073042 (2021).
- [33] T. Das, M. Karczewski, A. Mandarino, M. Markiewicz, B. Woloncewicz, and M. Żukowski, *Remarks about Bell-nonclassicality of a single photon*, Phys. Lett. A **435**, 128031 (2022).
- [34] T. Das, M. Karczewski, A. Mandarino, M. Markiewicz, M., B. Woloncewicz, and M. Żukowski, *Comment on ‘Single particle nonlocality with completely independent reference states’*, New J. Phys. **24**, 038001 (2022).
- [35] T. Das, M. Karczewski, A. Mandarino, M. Markiewicz, and M. Żukowski, *Optimal Interferometry for Bell Nonclassicality Induced by a Vacuum–One-Photon Qubit*, Phys. Rev. Appl. **18**, 034074 (2022).
- [36] R. Horodecki, P. Horodecki, M. Horodecki, and K. Horodecki, *Quantum entanglement*, Rev. Mod. Phys. **81**, 865 (2009).
- [37] N. Brunner, D. Cavalcanti, S. Pironio, V. Scarani, and S. Wehner, *Bell nonlocality*, Rev. Mod. Phys. **86**, 419 (2014).
- [38] D. V. Reddy, R. R. Nerem, S. W. Nam, R. P. Mirin, and V. B. Verma, *Superconducting nanowire single-photon detectors with 98% system detection efficiency at 1550 nm*, Optica **7**, 1649 (2020).
- [39] A. E. Lita, A. J. Miller, and S. W. Nam, *Counting near-infrared single-photons with 95% efficiency*, Opt. Express **16**, 3032 (2008).
- [40] M. Giustina, A. Mech, S. Ramelow, B. Wittmann, J. Kofler, J. Beyer, A. Lita, B. Calkins, T. Gerrits, S. W. Nam, R. Ursin, and A. Zeilinger, *Bell violation using entangled photons without the fair-sampling assumption*, Nature **497**, 227 (2013).
- [41] M. Giustina, M. A. Versteegh, S. Wengerowsky, J. Handsteiner, A. Hochrainer, K. Phelan, F. Steinlechner, J. Kofler, J.-Å. Larsson, C. Abellán, W. Amaya, V. Pruneri, M. W. Mitchell, J. Beyer, T. Gerrits, A. E. Lita, L. K. Shalm, S. W. Nam, T. Scheidl, R. Ursin, B. Wittmann, and A. Zeilinger, *Significant-loophole-free test of Bell’s theorem with entangled photons*, Phys. Rev. Lett. **115**, 250401 (2015).
- [42] D. Chruściński and A. Jamiołkowski, *Geometric phases in classical and quantum mechanics* (Springer, 2004).
- [43] M. Stobińska, A. Buraczewski, M. Moore, W. R. Clements, J. J. Renema, S. W. Nam, T. Gerrits, A. Lita, W. S. Kolthammer, A. Eckstein, I. A. Walmsley, *Quantum interference enables constant-time quantum information processing*, Sci. Adv. **5**, eaau9674 (2019).
- [44] K. Banaszek and K. Wódkiewicz, *Testing quantum nonlocality in phase space*, Phys. Rev. Lett. **82**, 2009 (1999).
- [45] K. Wódkiewicz, *Nonlocality of the Schrödinger cat*, New J. Phys. **2**, 21 (2000).
- [46] A. Kuzmich, I. A. Walmsley, and L. Mandel, *Violation of a Bell-type inequality in the homodyne measurement of light in an Einstein-Podolsky-Rosen state*, Phys. Rev. A **64**, 063804 (2001).
- [47] H. Jeong, W. Son, M. S. Kim, D. Ahn, and Č. Brukner, *Quantum nonlocality test for continuous-variable states with dichotomic observables*, Phys. Rev. A **67**, 012106 (2003).
- [48] S.-W. Lee and H. Jeong, *High-dimensional Bell test for a continuous-variable state in phase space and its robustness to detection inefficiency*, Phys. Rev. A **83**, 022103 (2011).
- [49] M. E. Mycroft, T. McDermott, A. Buraczewski, and M. Stobińska, *Proposal for the distribution of multiphoton entangle-*

- ment with optimal rate-distance scaling, *Phys. Rev. A* **107**, 012607 (2023).
- [50] P. Sekatski, N. Sangouard, M. Stobińska, F. Bussières, M. Afzelius, and N. Gisin, *Proposal for exploring macroscopic entanglement with a single photon and coherent states*, *Phys. Rev. A*, **86**, 060301 (2012).
- [51] M. G. A. Paris, *Displacement operator by beam splitter*, *Phys. Lett. A* **217**, 78 (1996).
- [52] A. I. Lvovsky and M. G. Raymer, *Continuous-variable optical quantum-state tomography*, *Rev. Mod. Phys.* **81**, 299 (2009).
- [53] M. A. Nielsen and I. L. Chuang, *Quantum computation and quantum information* (Cambridge University Press, 2010).
- [54] S. J. Summers and R. Werner, *Maximal violation of Bell's inequalities is generic in quantum field theory*, *Commun. Math. Phys.* **110**, 247 (1987).
- [55] A. Gheorghiu, P. Wallden, and E. Kashefi, *Rigidity of quantum steering and one-sided device-independent verifiable quantum computation*, *New J. Phys.* **19** 023043 (2017).
- [56] M. G. Dastidar and G. Sarbicki, *Detecting entanglement between modes of light*, *Phys. Rev. A* **105**, 062459 (2022).